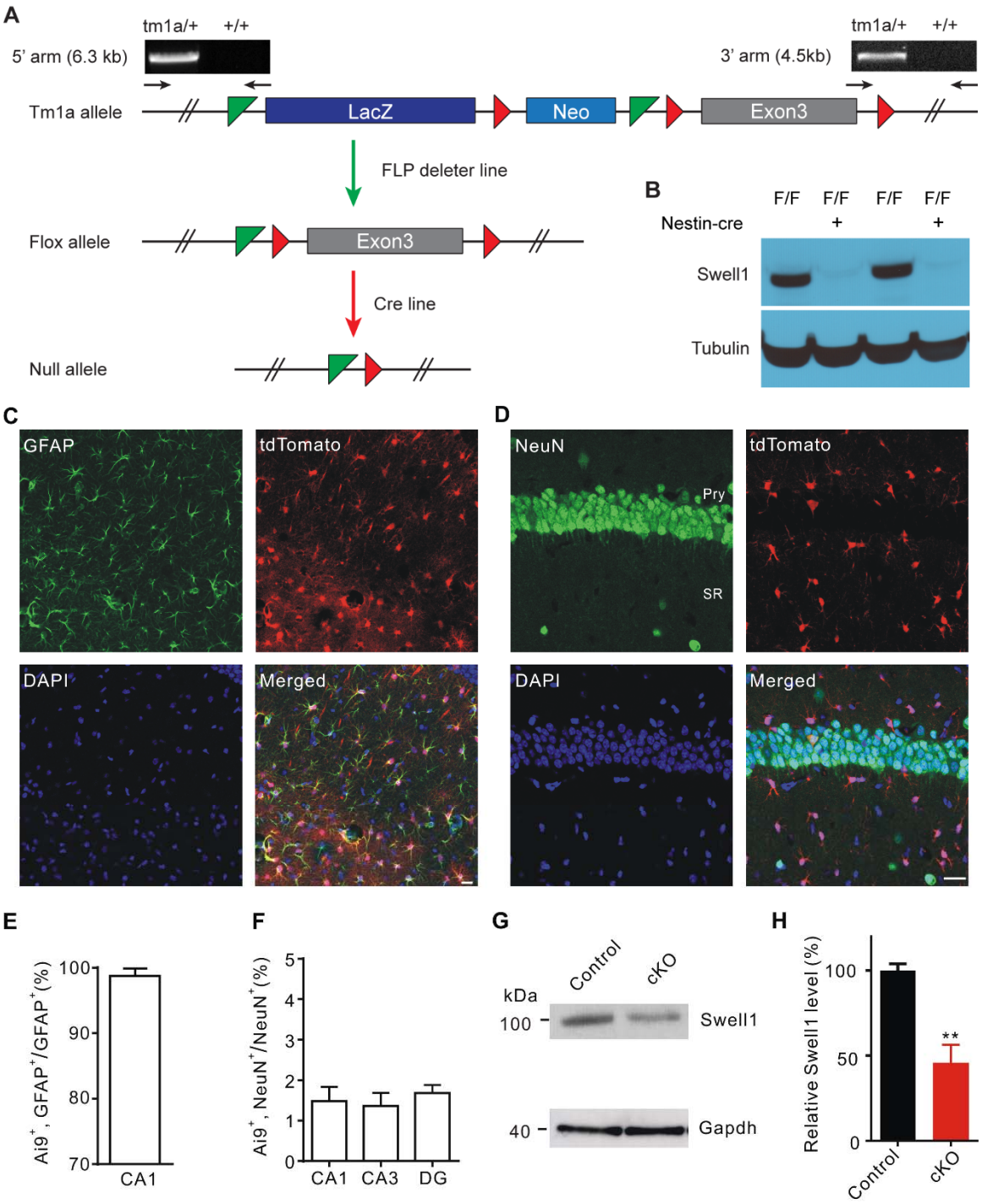

Figure S1. Generation and characterization of *Swell1* conditional knockout mice, Related to Figure 1 and 3.

(A) Targeting strategy of Swell1 genomic locus. Long-range PCRs confirmed the correct targeting. Cre-mediated recombination is expected to delete exon 3 and create a null allele.

(B) Western blot confirms loss of Swell1 protein in brain lysates prepared from *Swell1*$^{F/F}$ and *Swell1*$^{F/F}$*; Nestin-cre* mice.

(C and D) Representative images of GFAP (C) and NeuN (D) immunostaining in the hippocampus of *mGFAP-cre; Ai9* mice. Scale bar, 20 μm. The pyramidal cell layer (Pyr) and stratum radiatum (SR) are indicated.

(E) Percentage of colocalization between GFAP and tdTomato in the hippocampus of *mGFAP-cre; Ai9* mice. n = 12 slices from 6 mice.

(F) Percentage of colocalization between NeuN and tdTomato in the hippocampus of *mGFAP-cre; Ai9* mice. DG, dentate gyrus. n = 12 slices from 6 mice.

(G) Representative western blots from hippocampus lysates indicate a significant reduction of Swell1 protein in *Swell1* cKO mice.

(H) Quantification of Swell1 western blots. Swell1 was normalized by the loading control Gapdh. n = 3 pairs of mice. Student's t test, ** $p < 0.01$.

Data are reported as mean ± SEM.

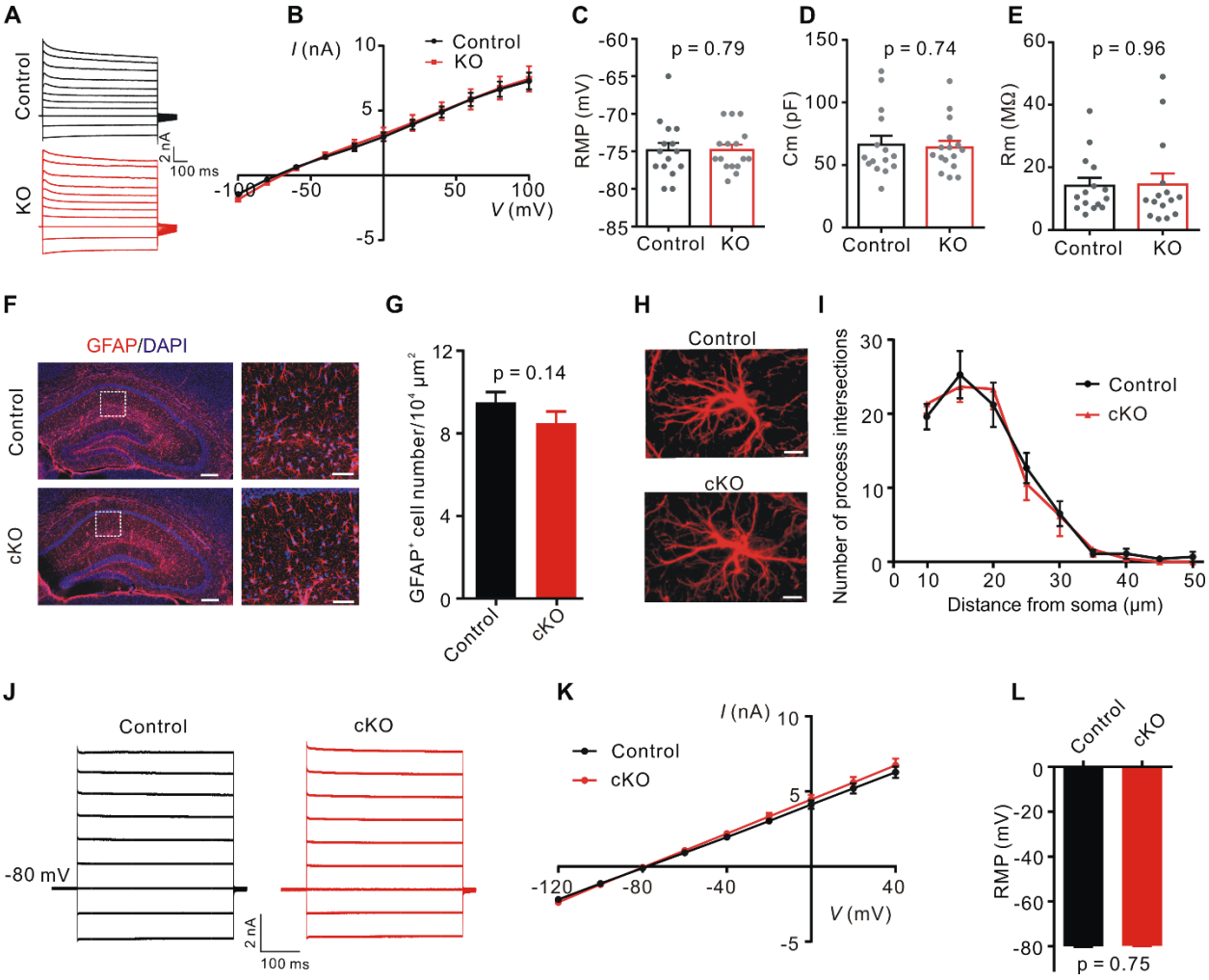

Figure S2. Astrocytes with *Swell1* deletion have normal electrophysiological properties, cell number and morphology, Related to Figure 1 and 3.

(A) Representative whole-cell currents recorded by voltage step (−100 mV to +100 mV, step 20 mV) in control and *Swell1* KO astrocytes.

(B) Average I/V plots for control and *Swell1* KO astrocytes, with representative traces shown in (A). n = 15 cells for each genotype.

(C-E) Quantification of the resting membrane potential (C), membrane capacitance (D), and membrane resistance (E). n = 15 cells for each genotype. Mann-Whitney test for (C) and (D), Student's t-test for (E).

(F) Representative images of GFAP immunostaining in the hippocampus of control and *Swell1* cKO mice. Enlarged images of the dotted areas were shown on the right. Scale bar: left, 200 μm; right, 50 μm.

(G) Quantifications of GFAP positive cells in the stratum radiatum region of hippocampus. n = 9 slices of 3 mice for each genotype. Mann-Whitney test.

(H) Representative images of single GFAP positive astrocyte. Z-stacks with 1 μm step were used to obtain the astrocyte processes. Scale bar, 5 μm.

(I) Quantification of astrocyte process intersections measured by Sholl analysis. n = 10 cells from 3 mice for control; n = 9 cells from 3 mice for *Swell1* cKO.

(J) Representative whole-cell currents recorded by voltage step (−120 mV to +40 mV, step 20 mV) in control and *Swell1* cKO hippocampal astrocytes.

(K) The corresponding current-voltage relationships for the recordings shown in (J). n = 12 cells from 4 mice for each genotype.

(L) Quantification of the resting membrane potentials (RMP) of astrocytes. n = 12 cells from 4 mice for each genotype. Student's t test.

Data are reported as mean ± SEM.

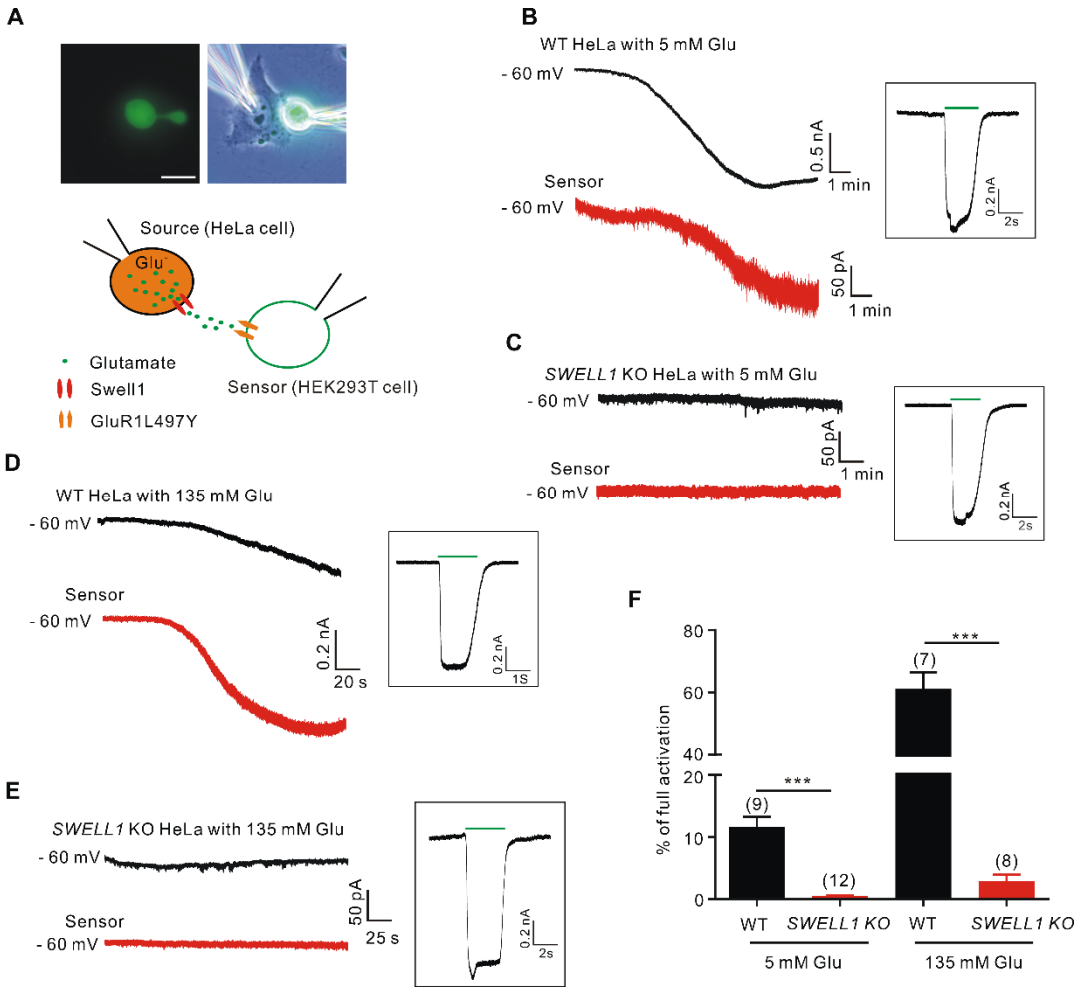

Figure S3. Glutamate release through VRAC in HeLa cells, Related to Figure 2.

(A) Top, representative images of sniffer-patch technique. Scale bar, 20 μm. Bottom, schematic illustration of sniffer-patch technique.

(B-E) Representative current traces recorded at −60 mV from source cell and sensor cell. The inward current in HeLa cell indicates VRAC activation. The inward current in the sensor cell indicates the detection of glutamate release from the nearby HeLa cell with 5 mM (B and C) or 135 mM (D and E) glutamate internal solution. After the experiment, full current activation in the sensor cell (inset) was recorded by bath application of 5 mM glutamate (green line).

(F) Quantification (mean ± SEM) of the percentage of full activation in each indicated condition. Cell number are indicated. Mann-Whitney test, *** $p < 0.01$.

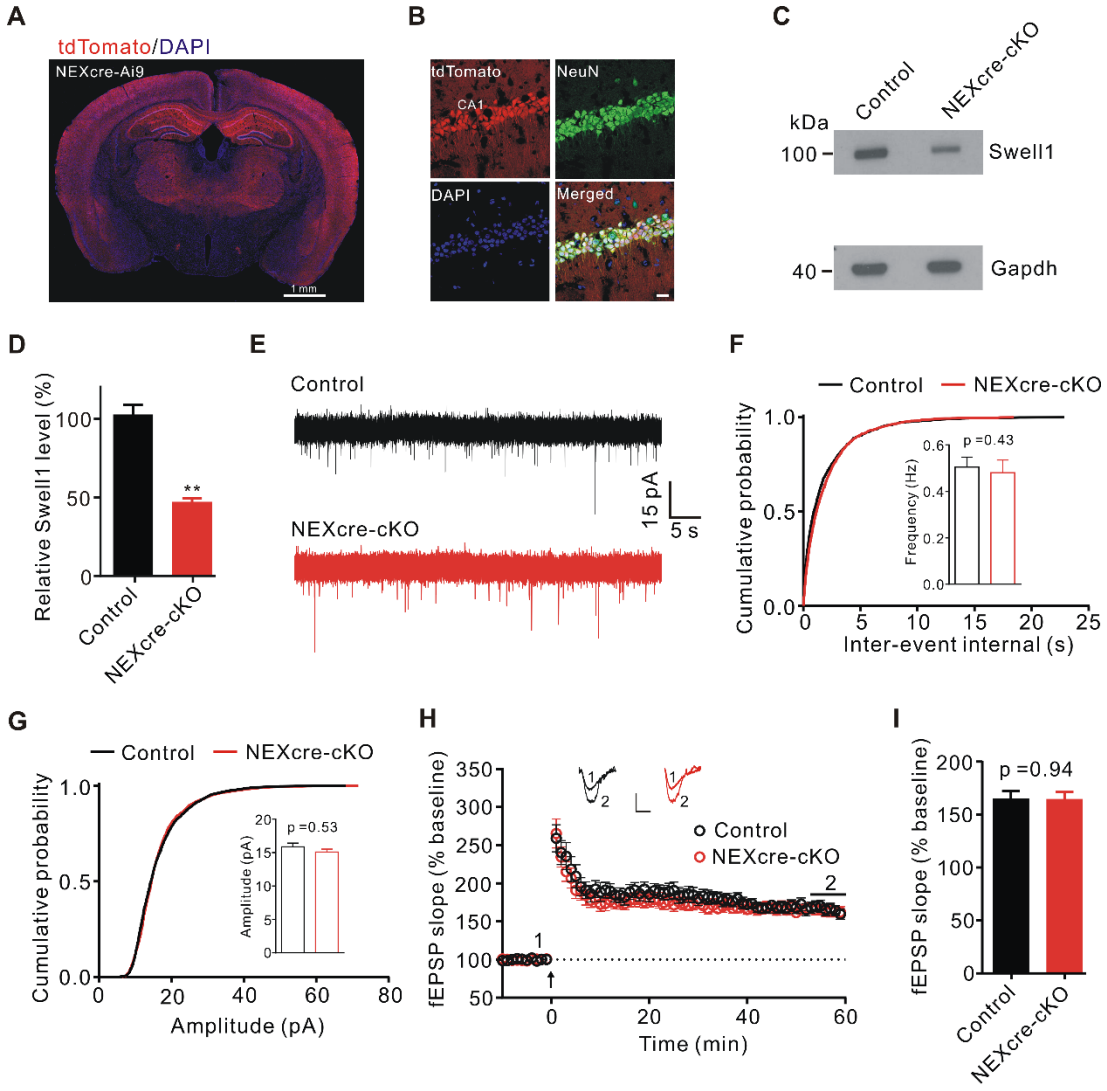

Figure S4. Glutamatergic synaptic transmission and LTP are normal in *Swell1*$^{F/F}$*; NEX-cre* mice, Related to Figure 3.

(A) Representative coronal section of *NEX-cre; Ai9* mcie.

(B) In hippocampal CA1, the Cre-mediated recombination is restricted to pyramidal neurons. Scale bar, 20 μm.

(C) Representative western blots of Swell1 protein from hippocampus lysates.

(D) Quantification of western blots. Swell1 was normalized by the loading control Gapdh. n = 3 pairs of mice. Student's t-test, ** $p < 0.01$.

(E) Representative traces of mEPSCs recorded from hippocampal CA1 neurons of control and NEXcre-cKO slices.

(F) Quantification of mEPSC frequency and cumulative probability of the inter-event intervals. n = 24 cells from 6 mice for each genotype. Mann-Whitney test.

(G) Quantification of mEPSC amplitude and cumulative probability of the amplitudes. n = 24 cells from 6 mice for each genotype. Mann-Whitney test.

(H) TBS-induced LTP at SC-CA1 synapses in control and NEXcre-cKO mice. Normalized fEPSP slopes were plotted every 1 min. Arrow indicates LTP induction. Sample traces represent fEPSPs taken before (1) and 50 min after TBS stimulation (2). Scale bars represent 0.5 mV (vertical), 5 ms (horizontal).

(I) Summary of experiments shown in (H). The amplitude of fEPSP slopes were averaged during 55-60 min after the stimulation. n = 14 slices from 5 mice for control; n = 15 slices from 6 mice for NEXcre-cKO. Student's t tests.

Data are reported as mean ± SEM.

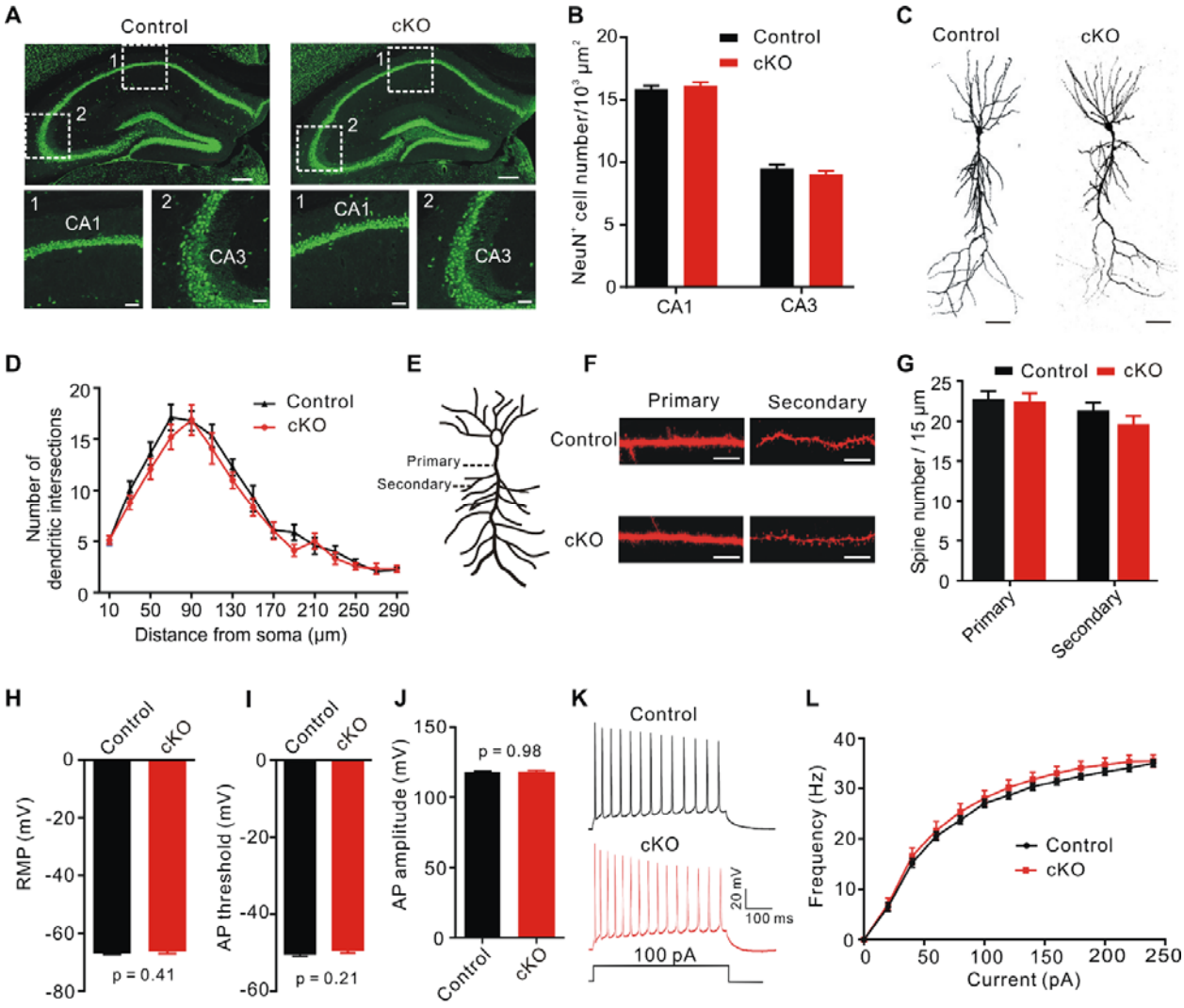

Figure S5. Normal neuron cell number, morphology, spine number and electrophysiological properties in the hippocampus of *Swell1* cKO mice, Related to Figure 3.

(A) Representative images of NeuN immunostaining in the hippocampus of control and *Swell1* cKO mice. The higher magnification of CA1 and CA3 regions (dotted box) is shown on the bottom. Scale bar: top, 200 μm; bottom, 50 μm.

(B) Quantification of NeuN positive cells in hippocampal CA1 and CA3 regions. n = 9 slices of 3 mice for each genotype. Two-way ANOVA, no significant difference was detected.

(C) Representative biocytin labeled CA1 pyramidal neurons. Scale bar, 50 μm.

(D) Quantification of neuronal dendritic intersections revealed by Sholl analysis. n = 10 cells from 5 mice for control; n = 15 cells from 6 mice for *Swell1* cKO.

(E) Schematic illustration of primary and secondary dendrites of hippocampal CA1 pyramidal neuron.

(F) Representative images of primary and secondary dendritic spine from biocytin labeled CA1 pyramidal neuron. Scale bar, 10 μm.

(G) Quantification of spine numbers in (F). n = 13 cells from 5 mice for each genotype. Two-way ANOVA, no significant difference was detected.

(H-J) Quantification of the resting membrane potential (H), action potential threshold (I), and action potential amplitude (J). n = 23-26 cells from 6 mice for each genotype. Student's t test.

(K) Representative traces of action potentials in CA1 pyramidal neurons evoked by depolarizing current of 100 pA.

(L) Summarized results of firing rate under increasing step currents. n = 23 cells from 6 mice for each genotype. Two-way ANOVA, no significant difference was detected.

Data are reported as mean ± SEM.

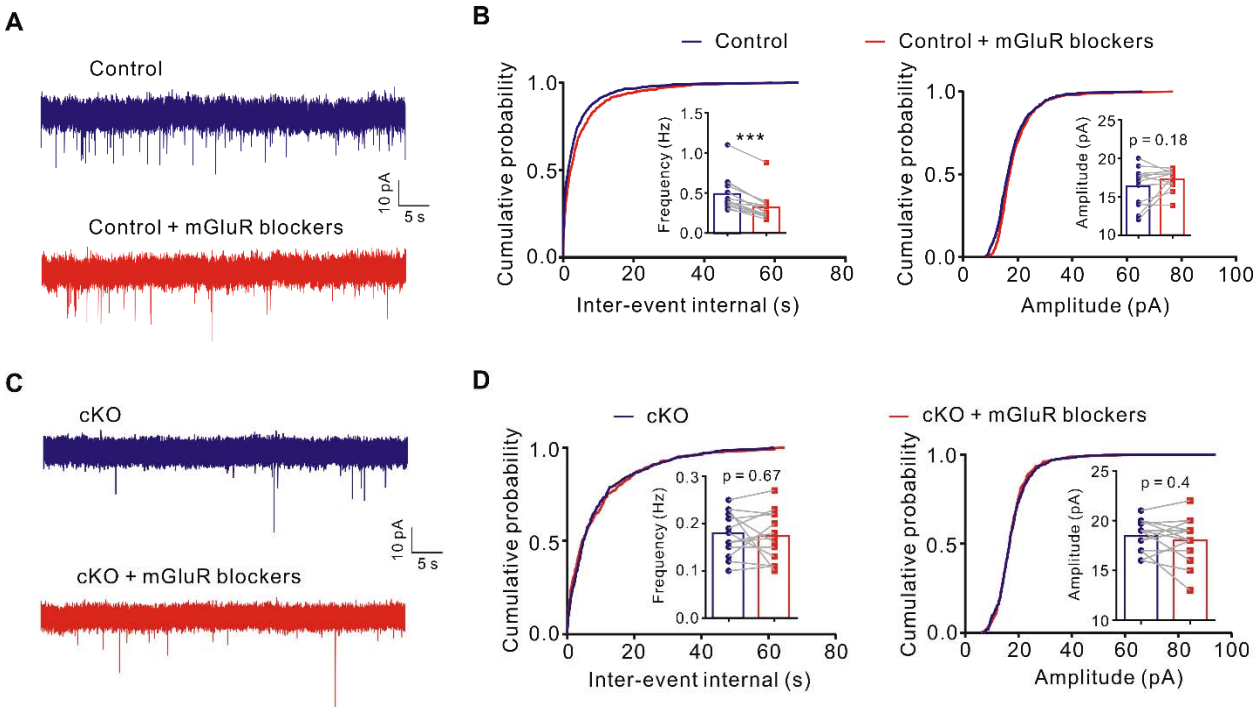

Figure S6. Involvement of mGluR hypofunction in the impairment of synaptic transmission in *Swell1* cKO mice, Related to Figure 5.

(A) Representative traces of mEPSCs recorded from hippocampal CA1 neurons of control mice before and after group I mGluRs antagonists (MPEP 50 μM and LY367385 100 μM) treatment.

(B) Cumulative probability plots of mEPSCs inter-event intervals (left) and amplitudes (right). n = 14 cells from 6 mice. Wilcoxon matched-pairs signed rank test, *** $p < 0.001$.

(C) Representative traces of mEPSCs recorded from hippocampal CA1 neurons of *Swell1* cKO mice before and after group I mGluRs antagonists (MPEP and LY367385) treatment.

(D) Cumulative probability plots of mEPSCs inter-event intervals (left) and amplitudes (right). n = 13 cells from 5 mice. Paired Student's t-test.

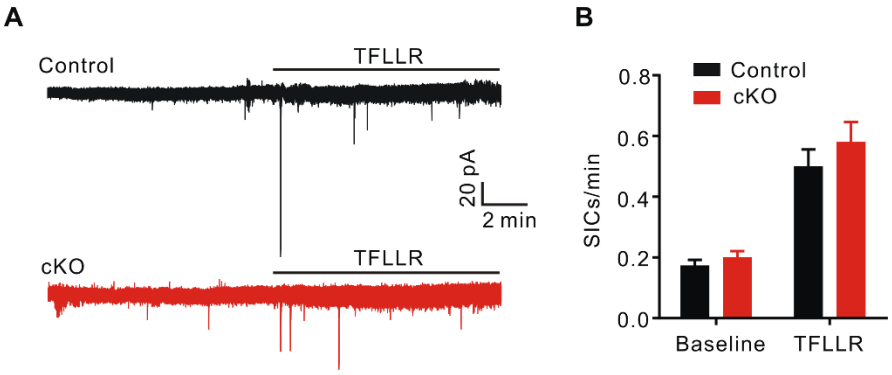

Figure S7. Slow inward currents (SICs) evoked by astrocytic PAR-1 receptor activation are normal in *Swell1* cKO mice, Related to Figure 7.

(A) Representative traces of SIC recordings from hippocampal CA1 pyramidal neurons induced by the application of PAR-1 agonist TFLLR (30 μM).

(B) SIC frequency for control (n = 10 cells from 5 mice) and *Swell1* cKO (n = 11 cells from 5 mice) before and after TFLLR application. Two-way ANOVA, no significant difference was detected.

Data are reported as mean ± SEM.